

GenLit: Reformulating Single-Image Relighting as Video Generation

Shrisha Bharadwaj* Haiwen Feng*,[†] Victoria Abrevaya Michael J. Black

Max Planck Institute for Intelligent Systems, Tübingen, Germany

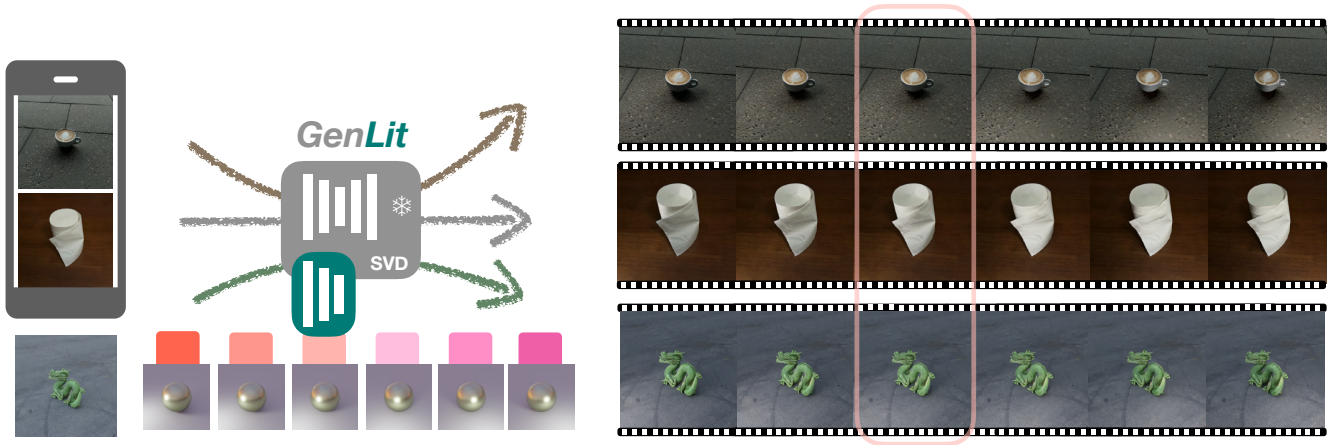


Figure 1. We introduce **GenLit**, a new framework for single image relighting. We reformulate the task as image-to-video generation, keeping the scene and the object in the image static while generating the lighting changes. We enhance the image-to-video model with interpretable control signals by fine-tuning on a small synthetic dataset. Despite being trained on a limited dataset and fine-tuned in a supervised manner, GenLit can convincingly relight phone-captured images.

Abstract

Manipulating the illumination within a single image represents a fundamental challenge in computer vision and graphics. This problem has been traditionally addressed using inverse rendering techniques, which require explicit 3D asset reconstruction and costly ray tracing simulations. Meanwhile, recent advancements in visual foundation models suggest that a new paradigm could soon be practical and possible – one that replaces explicit physical models with networks that are trained on massive amounts of image and video data. In this paper, we explore the potential of exploiting video diffusion models, and in particular Stable Video Diffusion (SVD), in understanding the physical world to perform relighting tasks given a single image. Specifically, we introduce GenLit, a framework that distills the ability of a graphics engine to perform light manipulation into a video generation model, enabling users to directly insert and manipulate a point light in the 3D world within a given image and generate the results directly as a video sequence. We find that a model fine-tuned on only a small

synthetic dataset (270 objects) is able to generalize to real images, enabling single-image relighting with realistic ray tracing effects and cast shadows. These results reveal the ability of video foundation models to capture rich information about lighting, material, and shape. Our findings suggest that such models, with minimal training, can be used for physically-based rendering without explicit physically asset reconstruction and complex ray tracing. This further suggests the potential of such models for controllable and physically accurate image synthesis tasks.

1. Introduction

Changing the illumination of the world inside a single image has practical applications in graphics and computational photography. This task, however, is inherently complex, as it is an ill-posed problem with multiple ambiguities related to the source light and albedo, lack of depth information, and insufficient prior knowledge of the materials. A common solution involves using an *inverse graphics* approach [1, 24], where explicit 3D assets for physics-based rendering (PBR) are recovered, including ge-

*Equal contribution, listed alphabetically. [†] Corresponding author.

ometry, material properties, and scene illumination, which are then re-rendered under novel lighting conditions. A good simulation of lighting effects requires not only a precise estimation of the 3D geometry and material properties (e.g., spatially-varying bi-directional reflectance distribution functions (SVBRDFs)), but also an accurate reproduction of complex light-matter interactions such as shadow casting and ray bouncing. Recovering all of this is difficult, error prone, and computationally expensive.

Recent progress in image and video foundation models [5, 37, 40, 53] suggests that a new paradigm for inverse rendering is possible, where the explicit PBR asset reconstruction is replaced by an image encoder and conditioning module, and complex ray tracing interactions are replaced by the generative model itself. The extensive training data behind such models enables them to directly learn and recreate real-world images at a pixel level, eliminating the need for *explicit* physics-based representations. Video diffusion models, in particular, have shown evidence of 3D understanding [4, 42] and can generate temporally consistent video that maintains the invariance of scene attributes, given only a single image as input. This suggests that these models have a significant understanding of the physical world, and can reason about and understand material properties as well as light-matter interactions. Thus, we ask the question: **Can we reformulate the single-image relighting problem as a controllable video synthesis task, by exploiting the physical understanding ability of video foundation models?**

In this work, we explore whether video diffusion models have sufficient understanding of the physical world to act as an implicit graphics engine to solve the task of single-image light manipulation. Here we focus on the case of relighting using a single point light source with fine-grained control over its position and intensity. We call our method **GenLit**, which performs generative relighting by enhancing an image-to-video model (Stable Video Diffusion (SVD) [4, 5]) with an interpretable control signal [53]. More specifically, GenLit takes a single image and generates a video of a moving light that is controlled by a 5D vector, which includes the point light’s 3D location, intensity, and the ambient light’s intensity. Unlike existing works that use pixel-aligned control signals [23, 51, 53, 54], ours corresponds directly to the world coordinate system of the scene, providing fine-grained and continuous control over the light source. To train our method we design a synthetic dataset dubbed OBJAVERSE-GENLIT, made of 270 objects sourced from Objaverse [9].

We evaluate GenLit on out-of-distribution scenarios through systematic experiments on both synthetic and real datasets, including the MIT Multi-Illumination dataset [30]. Our results show that GenLit can synthesize convincing shape- and light-appropriate shadows that generalize to unseen objects as well as phone-captured images. This indi-

cates that the model possesses an adequate level of physical understanding, and can potentially serve as an implicit rendering engine once it is fine-tuned for controllable synthesis. This investigation further reveals that video foundation models have sufficiently rich understanding of light, materials, and shape to support single-image controllable relighting, without the need to explicitly capture and design PBR assets (geometry, material, albedo, etc.) or perform expensive ray-tracing to model effects such as indirect illumination. Moreover, compared to state-of-the-art single-image relighting methods [49, 54, 57], we obtain significantly higher scores in both synthetic and real datasets.

In summary, we introduce a new framework that distills the ability to relight a single image with a point light from data rendered by a graphics engine, to a pre-trained image-to-video generative model, and the finetuned system generalizes to in-the-wild images. This illustrates how video diffusion models have a sufficient understanding of the world to serve as an implicit graphics engine for the task of single-image light manipulation. We will release the training code, pre-trained weights, and the OBJAVERSE-GENLIT dataset.

2. Related Work

Our work is centered on manipulating the light given only a single image. Hence, we focus our discussion on methods that do single-image relighting, either via explicit inverse rendering of geometry and materials, or via end-to-end learning using neural methods. Finally, we discuss work on controllable synthesis with diffusion models.

2.1. Inverse rendering

Given a single image, inverse rendering approaches estimate geometry, material and illumination of a scene, which can then be used to re-render the scene under novel lighting. Early work employs optimization-based approaches along with priors [1] to estimate albedo, reflectance and illumination, whereas recent approaches employ deep neural networks to estimate these for indoor [24, 25, 38, 44] or outdoor [50] scenes, trained either with self-supervision or with curated synthetic datasets. The majority of prior work cannot handle objects with complex, spatially varying BRDFs from only a single image, as they assume diffuse materials. Recent work [3, 13] leverage foundational generative priors to tackle the generalization issue, however their extracted intrinsic representations are limited in terms of material properties. Our goal, in contrast, is to leverage the broad physical understanding ability of image-to-video models, and to achieve zero-shot generalization in the case of image relighting.

2.2. Neural Relighting with Priors

An alternative to explicit reconstruction is to use neural methods, either for direct relighting or as priors. Sev-

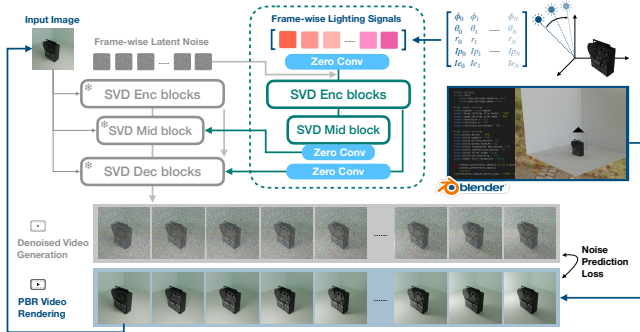


Figure 2. **Overview.** We use Blender to generate synthetic videos showing a point light in motion within a static scene. The first frame is fed to the generative branch (grey) as conditioning input, while per-frame lighting signals (5D vector) are provided as global information to the control branch (green). The features of the control branch are conditioned on the generative branch, enabling GenLit to generate a video of the input image where the lighting is controlled.

eral works use expensive light-stage setups [28, 31, 35, 36, 39] to learn data-driven priors with neural networks, or use GAN-based models [10, 34] and massive in-the-wild datasets to achieve better generalization. However, they are class-specific and cannot be easily extended to arbitrary objects. With the rise of diffusion models, several works have proposed solutions for relighting that leverage diffusion priors, *e.g.* estimate HDR maps [27, 32], insert objects [26], delight [8] given an image, or hallucinate artistic PBR materials for a given 3D mesh and text description [7, 11, 41, 56]. The following works [2, 23, 51] aim to control the lighting of an image generated by a text-to-image model. Bashkirova *et al.* [2] focus on class conditional control and are restricted to 12 lighting directions. Kocsis *et al.* [23] and Kangle *et al.* [51] are based on ControlNet [53] and control the lighting with pixel-aligned conditioning. While [23] propose a Shading Module to predict the shading of a given image, [51] use Blender to estimate radiance hints and use them as control signals respectively. However, neither are directly comparable to GenLit as [23] are based on outdoor large scenes and [51] handles images generated by text.

Concurrent works: IC-Light [54] based on text-to-image diffusion model is optionally designed to relight a single image given a background image, by blending the consistency of appearance. NeuralGaffer [20] performs single image relighting of an object using an img2img diffusion model where the conditioning signal is an HDR environment map. In contrast, we reformulate single image relighting as a video generation task, opt for a point light as the light source and obtain fine-grained control over the lighting. Moreover, we relight the image holistically includ-

ing the background and foreground object, which sets our method apart from concurrent works.

2.3. Controllable Video Synthesis with Diffusion Models

Recent advances in diffusion-based video generation methods have highlighted a significant focus on controllability, providing user-friendly techniques for generating videos under controlled conditions. With the emergence of methods used for fine-grained control on text-to-image (T2I) models [12, 29, 53], several extensions have been proposed to handle videos, *e.g.* for body-pose control [6, 17, 47], camera and object movement control [45], and last frame control [14, 19, 46, 52]. To the best of our knowledge, GenLit is the first work that investigates controllable relighting with an I2V generative model.

3. Method

Our goal is to investigate the level of physical understanding of an image-to-video (I2V) model, particularly Stable Video Diffusion (SVD) [4, 5], and to assess whether it can serve as an “implicit graphics renderer” given an input image. We achieve this by reformulating single-image relighting as video generation, where the scene and objects remain static while the illumination dynamically changes over time. Specifically, we train a controllable version of Stable Video Diffusion (Sec. 3.1) using a custom-designed control signal that continuously modifies the position and intensity of a point light source. Motivated by the fact that the ambient light might overpower the inserted point light in real images, we train our model to first “dim” the environment light, after which we introduce the motion of the point light according to the conditioning signal. Below, we describe our design to control the lighting of the generated video (Sec. 3.2) and conditioning mechanism (Sec. 3.3). An overview of our pipeline can be found in Fig. 2.

3.1. Background

Stable Video Diffusion [4, 5] (SVD) is a high-resolution image-to-video model based on Stable Diffusion [37], which introduces temporal blocks that learn to align the generated frames in a temporally consistent manner. Given a single image, SVD generates a video sequence of N frames, denoted by $\mathbf{x} = \{x^0, x^1, \dots, x^{N-1}\}$, where $N = 14$. This sequence is constructed through a denoising diffusion process where, at each denoising step t , a conditional 3D-UNet, Φ , is used to iteratively denoise the sequence: $\mathbf{x}_t = \Phi(\mathbf{x}_{t-1}, c)$. Here, c represents the conditioning information, which contains the CLIP [33] embedding of the single image input and the latents generated by stable diffusion’s VAE for the input image. This conditioning provides a consistent reference of the input image to the U-Net and

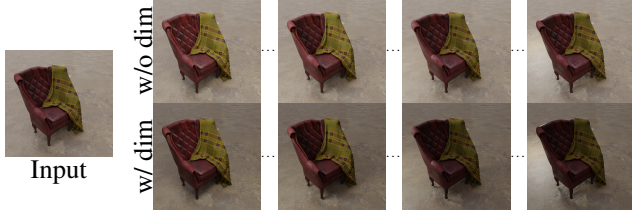


Figure 3. Importance of dimming at the beginning of the sequence. When the initial ambient light is very bright (“w/o dim”, top), the inserted point light gets overpowered. Our model instead dims the first few frames (“w/ dim”, bottom) to allow the inserted point light to be clearly visible.

helps in retaining the shape and material through the generation process when the scene light is changed.

3.2. Light Representation

3.2.1 Light Source

For the sake of simplicity, we choose a single point light as the light source as it gives us fine-grained control and can be defined by only two parameters: position and intensity. Moreover, a point light emits light uniformly and placing it close to an object results in sharp shadows. This allows to clearly investigate whether GenLit can generate effects such as local lighting and synthesized shadows (see *e.g.* Fig. 3).

3.2.2 Light Motion

Disentangling the lighting from a single image is a highly ill-posed problem, as multiple predictions can result in the same image. Naively inserting the point light without reducing the source light of the scene is suboptimal, as it is possible for the environment light to have a higher intensity in comparison to the point light. A demonstration of this effect is visualized in Fig. 3, top, where the relative intensity of the ambient environment light largely overpowers that of the point light. To tackle this, we introduce a novel strategy, in which the intensity of the environment light is first “dimmed” while simultaneously increasing the intensity of the point light (Fig. 3, bottom). This ensures that the point light is the dominant light and results in sharp cast shadows.

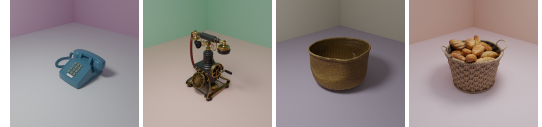
For each video, the object is static and the motion of light is as follows: for frames 1-4 the overall intensity is gradually dimmed and, starting at frame 2, the intensity of the point light is gradually increased until frame 4. From the fifth to the last frame, the point light is moved gradually to a new position. Specifically, we represent the motion of light as a sequence of 5D vectors, where for each frame i , the vector is given as: $\vec{l} = [(\phi_i, \theta_i, r_i, I_{p_i}, I_{e_i}); i = 1 \dots N]$, where I_{p_i} and I_{e_i} are scalar values representing the intensities of point light and environment light, respectively. The position of the point light is described in the polar coordi-



(a) shows uniqueness of the objects and the wall-area which reflects the color of the wall off the object.



(b) Demonstrates the construction of the open-area, where the textures from [21] enhance realism.



(c) shows object complexity and uniqueness even with overlapping categories “telephone” and “basket” class respectively.

Figure 4. **OBJAVERSE-GENLIT**: Overview of the dataset.

nate system, where θ and ϕ lie within the positive quadrant, and r is fixed. We discuss more details in SupMat.

3.3. Relighting as Controllable Video Synthesis

We use a pretrained Stable Video Diffusion [4, 5] (SVD) model that generates a video from a single image, and extend it with an approach similar to ControlNet [53]. We create the control signal by broadcasting \vec{l} (Sec. 3.2.2) onto an image $I \in R^{H \times W \times 5}$, which is fed to a trainable copy of the U-Net encoder, Ψ , which predicts control conditioning features. These features are added to SVD’s encoder Φ and directly influence the generation through the U-Net’s decoder. The pre-trained SVD model is frozen and only the weights of the control branch (Ψ) are updated. We fine-tune it by following the EulerEDM framework [22]. The controllable conditional denoising process is given as $\mathbf{x}_t = \Phi(\mathbf{x}_{t-1}, c, \Psi(I))$.

4. The OBJAVERSE-GENLIT Dataset

In this work, we aim to distill the interpretable light manipulation capabilities of traditional graphics engines into a video diffusion model. To this end we introduce OBJAVERSE-GENLIT, a novel dataset specifically designed for our task. OBJAVERSE-GENLIT consists of synthetic videos where static objects are illuminated by a moving point light source, capturing diverse light-object interactions that are challenging to model. Each video consists of 14 frames, rendered using Blender 3.2.2, and features a unique static object positioned at the center of the scene. The object is observed from a fixed camera viewpoint, while a single point light moves around it, dynamically chang-

ing the illumination conditions. We describe OBJAVERSE-GENLIT in detail in the following paragraphs.

Objects. The objects in our videos are sourced from the Objaverse [9] dataset, which offers a diverse collection of 3D meshes and materials spanning 945 LVIS [15] category annotations. This dataset includes not only common categories like cars and chairs but also intricate and unconventional objects (see *e.g.* Fig. 4) that reflect real-world complexity. Each object is rendered from four orthogonal views, rotated by 0° , 90° , 180° , and 270° along the z-axis. Note that each of these views look very distinct from each other, effectively augmenting the dataset by a factor of four. (examples and details in SupMat).

Scene Settings: Wall-Area and Open-Area. We propose two settings to evaluate different aspects of the light-material interaction. The **wall-area** setting (Fig. 4a) is constructed with three planes, one serving as the ground floor and two forming walls that surround the object. This configuration emphasizes indirect lighting effects, where the partially enclosed environment allows light rays to bounce multiple times between the environment and the object. The **open-area** setting (Fig. 4b) is designed to simulate more realistic conditions, and is used to evaluate generalization to in-the-wild images. In this setup, objects are placed on a single textured ground plane with no surrounding walls, using textures sourced from CLEVRText [21]. This setting not only aids GenLit in generalizing to real-world images (Fig. 7) but also demonstrates its ability to model complex material interactions with light in open environments.

Light. To create varied ambient environments, we randomly select an HDRI map from a curated list of 26 [16] for each object and rotate it by 0° , 90° , 180° , or 270° along the y-axis. As described in Sec. 3.2.2, we gradually dim the ambient light by reducing the HDRI map’s intensity to up to 40% of its original value. The point light’s location is specified in polar coordinates with $\theta \in [-90^\circ, 90^\circ]$, $\phi \in [15^\circ, 80^\circ]$, and a fixed radius $r = 1.5$, ensuring the light remains frontal. All possible positions lie on a spherical shell within this range. We generate a grid of light locations by sampling M evenly distributed values and create horizontal, vertical, and diagonal light motions by interpolating between points. The point light’s intensity increases from 0 to 75 lumens (adjusted in Blender for realism). We refer to the combined process of dimming, inserting, and moving the light as a “trajectory”. Details discussed in SupMat.

Training and Testing Split. Objects: We train on 270 objects, each rendered from four views with 41 random

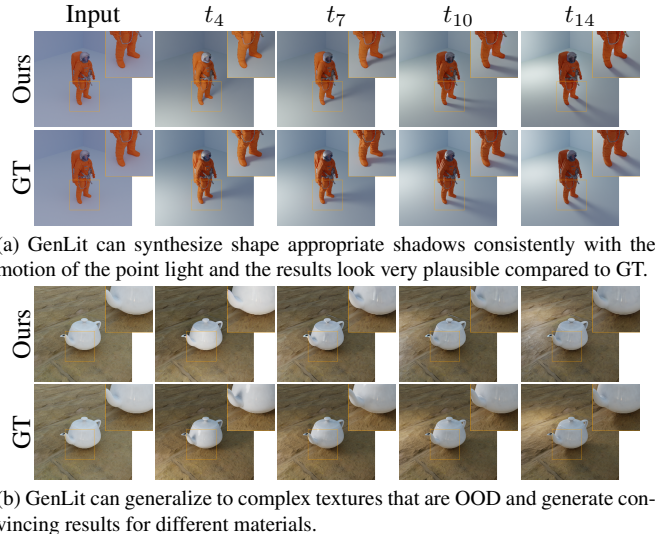


Figure 5. **Qualitative Evaluation** on the wall-area and open-area settings of OBJAVERSE-GENLIT. Each row displays frames sampled from a single video.

	RMSE ↓	LPIPS ↓	SSIM ↑	PSNR ↑
GENLIT-TEST_WALL-AREA	0.037	0.016	0.967	30.960
GENLIT-TEST_OPEN-AREA	0.047	0.096	0.734	30.588
500-OOD	0.041	0.014	0.942	28.770

Table 1. **Quantitative Evaluation** on the wall-area and open-area setting of OBJAVERSE-GENLIT.

light trajectories, totaling 44k videos and 620k frames. Scene: For the open-area setting, we select ground textures following the CLEVRText train/test split. Both the wall-area and open-area settings are independently used for training (see Sec. 5). Light: To keep training and testing point light locations distinct, we generate two disjoint sets of uniformly sampled values by setting $M = 128$ for training and $M = 64$ for testing. This ensures test light locations and motions are novel but remain within the bounds of θ and ϕ . We maintain the same intensity values so the model learns to reduce the source light effectively. For testing, we evaluate on the following scenarios:

1- GENLIT-TEST: This test set consists of 22 objects, each rendered from 4 views and 41 light trajectories, resulting in a total of 3.6k videos and 50k frames. Of these 22 objects, 6 are classic models commonly used in computer graphics (Armadillo, Nefertiti, Stanford Bunny, Teapot, XYZ Dragon, Teapot-2), which we manually verified are not part of the LVIS classification of Objaverse. Five objects belong to completely unseen LVIS categories compared to the training split, while the remaining objects share categories with the training set, they have significantly different geometries (see Fig. 4c). This test set is rendered in both the wall-area (GENLIT-TEST_WALL-AREA) and

open-area (GENLIT-TEST_OPEN-AREA) settings. Visualizations of all test set objects are included in SupMat.

2. 500-OOD: To test out-of-distribution (OOD) generalization to entirely unseen categories, we sample 500 unique categories from the LVIS classification, ensuring none of these were included in the training set. For each category, we sample one object and render it from four orthogonal views under two random light trajectories (compared to 41 in the previous test). Here we only use the wall-area setting, to carefully study the interaction of light with the shape of the object.

3. REAL DATA. To evaluate zero-shot generalization to real-world images, we capture photographs of various objects using an iPhone 15. These objects are placed on flat surfaces under ambient illumination, mimicking the open-area setting. We manually verified that none of the photographed objects appear in the training set, although some categories (e.g., coffee cup) overlap. Since this test set does not include relighting ground truth, it is intended solely for qualitative evaluation. An example of our captured data is shown in Fig. 7, column 1.

5. Evaluation

In this section, we conduct systematic controlled experiments as follows: First, we evaluate GenLit’s performance as an implicit graphics renderer by thoroughly evaluating the relighting quality on GenLit-Test in Sec. 5.1.1, and by comparing against state-of-the-art methods for single-image relighting in Sec. 5.1.2. Further, we investigate GenLit’s zero-shot generalization in Sec. 5.1.3 by evaluating on 500-OOD and then qualitatively evaluating on Real Data to investigate knowledge transfer from synthetic to real. Finally, we conduct evaluations on MIT Multi-Illum. Dataset [30] and show that GenLit can scale to real world captures containing multiple objects. The quantitative evaluations are measured using image-space metrics: Root Mean Squared Error (RMSE), perceptual loss (LPIPS) [55], structural similarity index measure (SSIM) [43] and PSNR against the ground truth images. Additional video results can be found in our [WEBPAGE](#).

5.1. Analysis on the OBJAVERSE-GENLIT Dataset

5.1.1 Analysis on Relighting Quality

We evaluate relighting extensively with the GenLit-Test for both wall-area and open-area and conduct quantitative evaluations on roughly 50k frames (Tab. 1). GenLit performs better on wall-area in comparison to open-area, as the latter has OOD textures [21] that have complex material properties. The goal of this analysis is to evaluate how well GenLit acts as an implicit graphics renderer, thus, our qualitative analysis is focused on verifying whether the generated shadows match the shape of the ob-

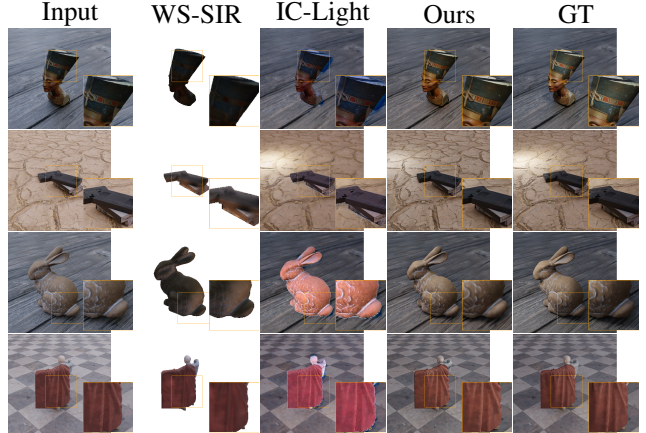


Figure 6. **Qualitative Evaluation: Baseline Comparisons** with IC-Light [54] and WS-SIR [49] on open-area dataset.

	RMSE ↓	LPIPS ↓	SSIM ↑	PSNR ↑
IC-Light	0.052	0.023	0.9729	40.023
WS-SIR	0.053	0.037	0.9618	40.213
Ours	0.018	0.009	0.9797	41.830

Table 2. **Quantitative Evaluation: Baseline Comparisons.** GenLit-Test_{open-area} evaluated only on the foreground object for fairness, with image-diffusion baseline IC-Light [54] and inverse rendering baseline WS-SIR [49].

ject, if the inserted point light location matches the ground truth, and the quality of the object materials.

Wall-Area setting. From Fig. 5a, we see that the synthesized shadows are very close to the ground truth; i.e., the legs of the astronaut have two separate shadows that move as the point light moves. Moreover, from columns 4 and 5, we see that the inserted point light is close to the walls, and as a result, the light bouncing off the walls increases the intensity of the point light within the closed region. These results show that GenLit can generate realistic interactions between the object and the walls by inserting the point light in plausible locations even for unseen objects.

Open-Area setting. From Fig. 5b, we see that GenLit can generate very realistic relighting for unseen complex materials like the ground plane even after changing the position of the light. Moreover, across the columns, we can see the teapot gets brighter when the light is in the front, and then dimmer as the light goes behind. Thus, GenLit can implicitly generate convincingly similar results as the ground truth which is generated explicitly with ray tracing and 3D assets.

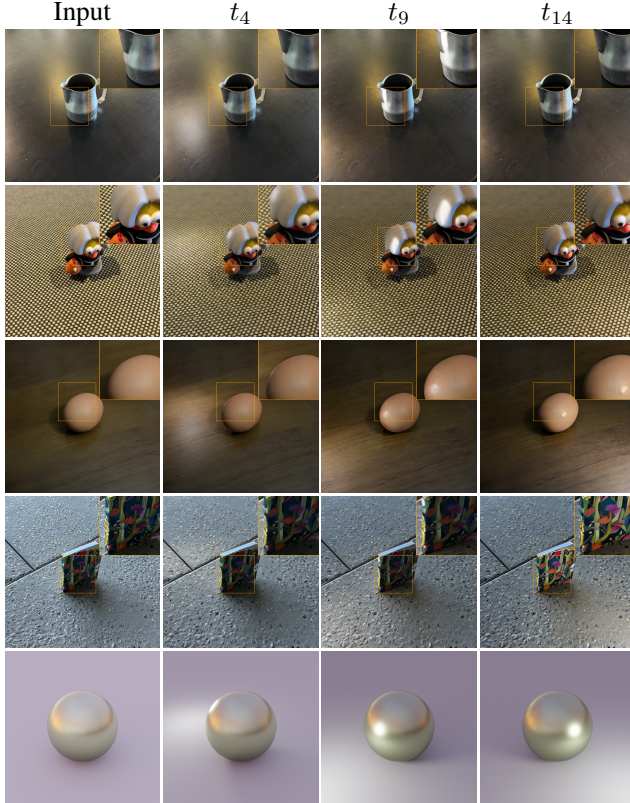


Figure 7. **Qualitative Evaluation: Generalization - Sim2Real.** All the input images are generated with the same light positions visualized on a synthetic metallic sphere in the last row for reference. GenLit generates very realistic renderings demonstrating remarkable generalization to phone captured images.

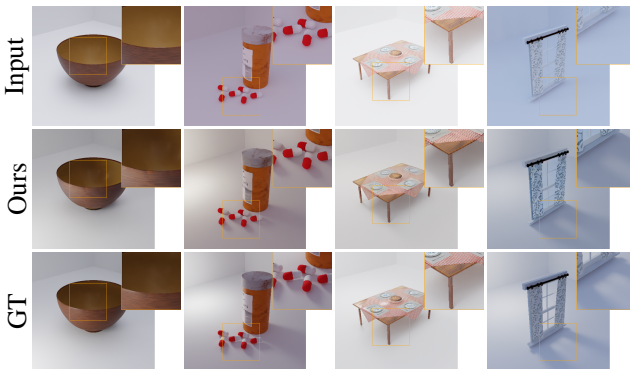


Figure 8. **Qualitative Evaluation: Generalization - 500-OOD.** GenLit can generalize effectively to unseen objects that are absent in the train set by synthesising shape-appropriate shadows.

5.1.2 Comparison with State-of-the-Art

We evaluate on GenLit-Test_{open-area} (Tab. 2) setting since the backgrounds are more realistic and OOD. We compare with the following methods that accept a single im-

age of a *single object* as input: (1) IC-Light [54] is built on control-net [53] and is designed to relight a foreground object by blending an input background image to achieve consistency in appearance. (2) WS-SIR [49] follows a conventional reconstruction+relighting pipeline based on a lambertian shading model and represent the light using spherical harmonics. Both of these methods differ significantly in construction as they represent different paradigms for relighting and we render the additional inputs required by the methods for relighting (details in SupMat).

From Fig. 6, we see that IC-Light struggles to retain the source color of the object after relighting. Moreover, as it is trained to blend foreground and background, the ground texture can act as an additional light source, with background colors bleeding onto the foreground. On the other hand, GenLit can retain the source color of the object very well (see *e.g.* row 3, 4). WS-SIR predicts noisy surface normals which leads to incorrect relighting (see *e.g.* row 2). Additionally, disentangling the light and albedo from a single image is non-trivial and their albedo estimates bake in the shading, making the relighting challenging. In contrast, GenLit acts as an implicit renderer and excels at handling local lighting effects (see *e.g.* row 1, 2).

5.1.3 Analysis on Generalization Ability

500-OOD: Generalization to Unseen Object Categories

We quantitatively evaluate (Tab. 1, row 3) on 500-OOD described in Sec. 4. The evaluations are performed using the same model that is *trained only on 270 objects*. As shown in Fig. 8, GenLit demonstrates a remarkable understanding of object shape by synthesizing plausible shadows for the concave bowl (col 1) and individual shadows for each capsule (col 2), indicating an understanding of object compositionality. Additionally, GenLit distinguishes between different materials, as seen in row 4, where it renders shadows only for the opaque curtain sections and not for the transparent window. This shows that GenLit is robust and can generalize to a wide spectrum of object shapes and materials.

Sim2Real: Generalization to Real Images

In Fig. 7, we show generalization of GenLit on *real images* captured on phone (Sec. 4) using the model trained on *open-area* which has only 270 *synthetic objects*. Interestingly, all the images show that GenLit can remarkably preserve the shape and synthesize plausible reflection for appropriate materials. For example, in row 1, the model can successfully synthesize specularities on the metal mug, indicating an implicit, semantic understanding that leads to a plausible relighting. Next, in row 5, the image of the book contains a strong shadow, despite which GenLit convincingly manipulates the light while retaining its texture properties and geometry, as well as the shadow on the ground. This im-

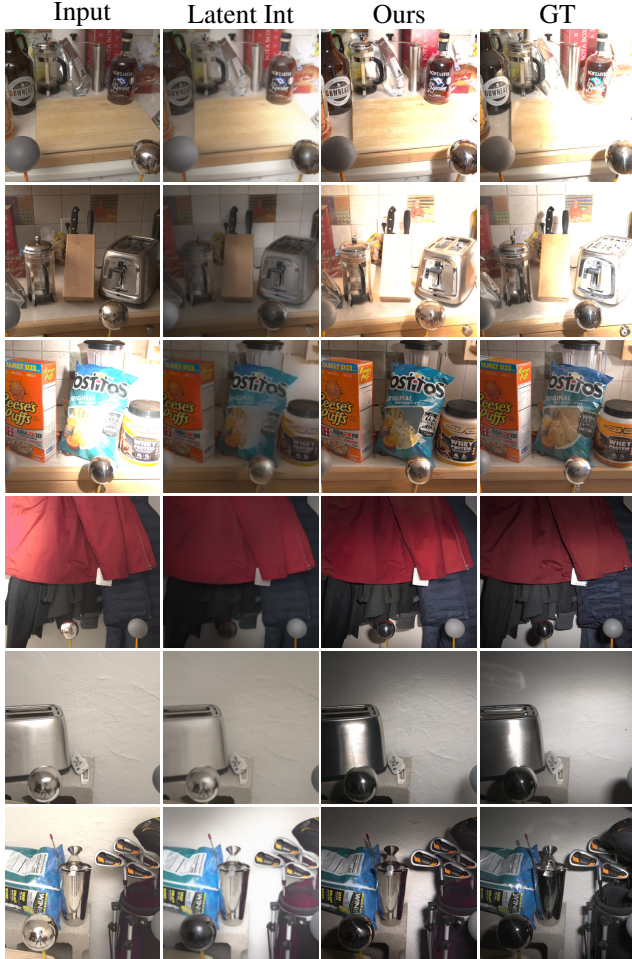


Figure 9. **Qualitative Evaluation: MIT Dataset - Baseline Comparison** with Latent-Intrinsics [57]. The results show that GenLit can generalize to large-scale scene with multiple cluttered objects.

plies that GenLit can synthesize these effects from a single image, implicitly, without underlying information about geometry or material assets.

5.2. Evaluation on MIT Multi-Illum. Dataset

To scale GenLit to large scenes, we train our method on the train split of the MIT Multi-Illumination Dataset [30], which contains a single mounted light source rotated in 25 lighting directions across 945 scenes. We adapt it to our setting by creating 25 video sequences that have continuous motion (described in SupMat). We conduct evaluations on the test split (Tab. 3) containing 30 scenes and compare with a state-of-the-art encoder-based method Latent Intrinsics [57]. From Fig. 9, we see that GenLit preserves scene details and synthesizes very realistic relighting effects compared to Latent Intrinsics. Primarily, from row 1 we see that as the light is very close to the camera, our prediction contains a bright spot, similar to the groundtruth where the

	RMSE ↓	LPIPS ↓	SSIM ↑	PSNR ↑
Lat. Intr.	0.1513	0.1526	0.7574	28.454
Ours	0.1129	0.1302	0.7623	28.974
SA-AE [18]	0.317	-	0.431	-
S3NET [48]	0.414	-	0.377	-
Lat. Intr	0.222	-	0.571	-
Ours	0.219	-	0.584	-

Table 3. **Quantitative Evaluation: MIT Multi-Illumn** comparing against Latent Intrinsics [57]. Top: additional metrics (PyTorch impl.). Bottom: Scores taken from Tab. 1 of [57] and metrics computed using the authors’ implementation for fairness.

input image has an ambient light source. Further, row 2 has an overexposed input image, but GenLit can still hallucinate the chips packet (empty), while latent intrinsics has a white artifact in the prediction. Finally, row 3, our result has a sharp specularity on the toaster that is not present in the input and is similar to the ground truth specularity. These results indicate that GenLit can scale exceptionally to large-scale real world scenes with cluttered objects.

6. Conclusions

In this work we investigated whether a video diffusion model, specifically Stable Video Diffusion (SVD), could serve as an implicit graphics renderer for relighting objects from a single image. By minimally supervising SVD with controllable signals for light position and intensity, our proposed approach, GenLit, can effectively perform complex light manipulation tasks. Our experiments demonstrate fine-tuning video diffusion models are a promising alternative to traditional image relighting pipelines.

GenLit generalizes from a limited synthetic training set of 270 objects to remarkably handle real-world images, demonstrating practical applicability and robustness. However, its reliance on a VQVAE encoder-decoder limits its ability to reproduce fine details, which is a drawback when precision is essential. Additionally, GenLit inherits the slow inference speeds typical of diffusion models, hindering its usability for real-time rendering.

Our work focuses on the simplified scenario of a single point light source. Future research should explore extending this approach to an HDRI map to fully alter the ambient environment of the scene.

We hope this study inspires further exploration of the physical modeling capabilities of foundational video generative models and their potential applications in image analysis and editing.

References

- [1] Jonathan T Barron and Jitendra Malik. Shape, illumination, and reflectance from shading. *IEEE transactions on pattern analysis and machine intelligence*, 37(8):1670–1687, 2014. 1, 2
- [2] Dina Bashkirova, Arijit Ray, Rupayan Mallick, Sarah Adel Bargal, Jianming Zhang, Ranjay Krishna, and Kate Saenko. Lasagna: Layered Score Distillation for Disentangled Object Relighting, 2023. [arXiv:2312.00833](https://arxiv.org/abs/2312.00833) [cs]. 3
- [3] Anand Bhattad, Daniel McKee, Derek Hoiem, and David Alexander Forsyth. Stylegan knows normal, depth, albedo, and more. *ArXiv*, abs/2306.00987, 2023. 2
- [4] Andreas Blattmann, Tim Dockhorn, Sumith Kulal, Daniel Mendelevitch, Maciej Kilian, Dominik Lorenz, Yam Levi, Zion English, Vikram Voleti, Adam Letts, et al. Stable video diffusion: Scaling latent video diffusion models to large datasets. *arXiv preprint arXiv:2311.15127*, 2023. 2, 3, 4
- [5] Andreas Blattmann, Robin Rombach, Huan Ling, Tim Dockhorn, Seung Wook Kim, Sanja Fidler, and Karsten Kreis. Align your latents: High-resolution video synthesis with latent diffusion models. In *IEEE Conference on Computer Vision and Pattern Recognition (CVPR)*, 2023. 2, 3, 4
- [6] Di Chang, Yichun Shi, Quankai Gao, Jessica Fu, Hongyi Xu, Guoxian Song, Qing Yan, Yizhe Zhu, Xiao Yang, and Mohammad Soleymani. Magicpose: Realistic human poses and facial expressions retargeting with identity-aware diffusion, 2024. 3
- [7] Rui Chen, Yongwei Chen, Ningxin Jiao, and Kui Jia. Fantasia3d: Disentangling geometry and appearance for high-quality text-to-3d content creation. In *Proceedings of the IEEE/CVF International Conference on Computer Vision (ICCV)*, pages 22246–22256, 2023. 3
- [8] Xi Chen, Sida Peng, Dongchen Yang, Yuan Liu, Bowen Pan, Chengfei Lyu, and Xiaowei Zhou. IntrinsicAnything: learning diffusion priors for inverse rendering under unknown illumination. In *European Conference on Computer Vision (ECCV)*, 2024. 3
- [9] Matt Deitke, Ruoshi Liu, Matthew Wallingford, Huong Ngo, Oscar Michel, Aditya Kusupati, Alan Fan, Christian Laforte, Vikram Voleti, Samir Yitzhak Gadre, et al. Objaverse-xl: A universe of 10m+ 3d objects. *Advances in Neural Information Processing Systems*, 36, 2024. 2, 5, 12
- [10] Boyang Deng, Yifan Wang, and Gordon Wetzstein. Lumigan: Unconditional generation of relightable 3d human faces. *arXiv preprint arXiv:2304.13153*, 2023. 3
- [11] Kangle Deng, Timothy Omernick, Alexander B Weiss, Deva Ramanan, Jun-Yan Zhu, Tinghui Zhou, and Maneesh Agrawala. FlashTex: fast relightable mesh texturing with LightControlNet. In *European Conference on Computer Vision (ECCV)*, 2024. 3
- [12] Johann-Friedrich Feiden Denis Zavadski and Carsten Rother. ControlNet-XS: Designing an efficient and effective architecture for controlling text-to-image diffusion models. 2023. 3
- [13] Xiaodan Du, Nicholas Kolkin, Greg Shakhnarovich, and Anand Bhattad. Generative models: What do they know? do they know things? let’s find out! *arXiv*, 2023. 2
- [14] Haiwen Feng, Zheng Ding, Zhihao Xia, Simon Niklaus, Victoria Abrevaya, Michael J. Black, and Xuaner Zhang. Explorative inbetweening of time and space. *ArXiv*, abs/2403.14611, 2024. 3
- [15] Agrim Gupta, Piotr Dollar, and Ross Girshick. LVIS: A dataset for large vocabulary instance segmentation. In *Proceedings of the IEEE Conference on Computer Vision and Pattern Recognition*, 2019. 5, 12
- [16] Poly Haven. Poly haven: Free high-quality 3d assets and hdris. <https://polyhaven.com/>, 2024. Accessed: 2024-11-13. 5
- [17] Li Hu, Xin Gao, Peng Zhang, Ke Sun, Bang Zhang, and Liefeng Bo. Animate anyone: Consistent and controllable image-to-video synthesis for character animation. *arXiv preprint arXiv:2311.17117*, 2023. 3
- [18] Zhongyun Hu, Xin Huang, Yaning Li, and Qing Wang. Saae for any-to-any relighting. In *Computer Vision – ECCV 2020 Workshops: Glasgow, UK, August 23–28, 2020, Proceedings, Part III*, page 535–549, Berlin, Heidelberg, 2020. Springer-Verlag. 8
- [19] Siddhant Jain, Daniel Watson, Eric Tabellion, Aleksander Holy’nski, Ben Poole, and Janne Kontkanen. Video interpolation with diffusion models. *ArXiv*, abs/2404.01203, 2024. 3
- [20] Haian Jin, Yuan Li, Fujun Luan, Yuanbo Xiangli, Sai Bi, Kai Zhang, Zexiang Xu, Jin Sun, and Noah Snavely. Neural gaffer: Relighting any object via diffusion. In *Conference on Neural Information Processing Systems (NeurIPS)*, 2024. 3
- [21] Laurynas Karazija, Iro Laina, and Christian Ruppel. ClevrTex: A Texture-Rich Benchmark for Unsupervised Multi-Object Segmentation. In *Thirty-fifth Conference on Neural Information Processing Systems Datasets and Benchmarks Track*, 2021. 4, 5, 6
- [22] Tero Karras, Miika Aittala, Timo Aila, and Samuli Laine. Elucidating the design space of diffusion-based generative models. In *Proc. NeurIPS*, 2022. 4
- [23] Peter Kocsis, Julien Philip, Kalyan Sunkavalli, Matthias Nießner, and Yannick Hold-Geoffroy. Lightit: Illumination modeling and control for diffusion models. In *CVPR*, 2024. 2, 3
- [24] Zhengqin Li, Mohammad Shafiei, Ravi Ramamoorthi, Kalyan Sunkavalli, and Manmohan Chandraker. Inverse rendering for complex indoor scenes: Shape, spatially-varying lighting and svbrdf from a single image. In *Proceedings of the IEEE/CVF Conference on Computer Vision and Pattern Recognition*, pages 2475–2484, 2020. 1, 2
- [25] Zhengqin Li, Jia Shi, Sai Bi, Rui Zhu, Kalyan Sunkavalli, Milovs Havsan, Zexiang Xu, Ravi Ramamoorthi, and Manmohan Chandraker. Physically-based editing of indoor scene lighting from a single image. *ECCV*, abs/2205.09343, 2022. 2
- [26] Ruofan Liang, Zan Gojcic, Merlin Nimier-David, David Acuna, Nandita Vijaykumar, Sanja Fidler, and Zian Wang. Photorealistic object insertion with diffusion-guided inverse rendering. In *European Conference on Computer Vision (ECCV)*, 2024. 3
- [27] Linjie Lyu, Ayush Tewari, Marc Habermann, Shunsuke Saito, Michael Zollhöfer, Thomas Leimkühler, and

- Christian Theobalt. Diffusion posterior illumination for ambiguity-aware inverse rendering. *ACM Transactions on Graphics*, 42(6), 2023. 3
- [28] Yiqun Mei, Yu Zeng, He Zhang, Zhixin Shu, Xuaner Zhang, Sai Bi, Jianming Zhang, HyunJoon Jung, and Vishal M Patel. Holo-relighting: Controllable volumetric portrait relighting from a single image. In *Proceedings of the IEEE/CVF International Conference on Computer Vision*, 2024. 3
- [29] Chong Mou, Xintao Wang, Liangbin Xie, Yanze Wu, Jian Zhang, Zhongang Qi, Ying Shan, and Xiaohu Qie. T2i-adapter: Learning adapters to dig out more controllable ability for text-to-image diffusion models. *arXiv preprint arXiv:2302.08453*, 2023. 3
- [30] Lukas Murmann, Michael Gharbi, Miika Aittala, and Fredo Durand. A multi-illumination dataset of indoor object appearance. In *2019 IEEE International Conference on Computer Vision (ICCV)*, 2019. 2, 6, 8
- [31] Rohit Pandey, Sergio Orts-Escolano, Chloe Legendre, Christian Haene, Sofien Bouaziz, Christoph Rhemann, Paul E Debevec, and Sean Ryan Fanello. Total relighting: learning to relight portraits for background replacement. *ACM Trans. Graph.*, 40(4):43–1, 2021. 3
- [32] Pakkapon Phongthawee, Worameth Chinchuthakun, Nontaphat Sinsunthithet, Varun Jampani, Amit Raj, Pramook Khungurn, and Supasorn Suwajanakorn. DiffusionLight: light probes for free by painting a chrome ball. In *Computer Vision and Pattern Recognition (CVPR)*, 2024. 3
- [33] Alec Radford, Jong Wook Kim, Chris Hallacy, Aditya Ramesh, Gabriel Goh, Sandhini Agarwal, Girish Sastry, Amanda Askell, Pamela Mishkin, Jack Clark, Gretchen Krueger, and Ilya Sutskever. Learning transferable visual models from natural language supervision. In *International Conference on Machine Learning*, 2021. 3
- [34] Anurag Ranjan, Kwang Moo Yi, Jen-Hao Rick Chang, and Oncel Tuzel. Facelit: Neural 3d relightable faces. In *Proceedings of the IEEE/CVF Conference on Computer Vision and Pattern Recognition*, pages 8619–8628, 2023. 3
- [35] Pramod Rao, Mallikarjun B R, Gereon Fox, Tim Weyrich, Bernd Bickel, Hans-Peter Seidel, Hanspeter Pfister, Wojciech Matusik, Ayush Tewari, Christian Theobalt, and Mohamed Elgharib. Vorf: Volumetric relightable faces. 2022. 3
- [36] Pramod Rao, Gereon Fox, Abhimitra Meka, Mallikarjun B R, Fangneng Zhan, Tim Weyrich, Bernd Bickel, Hans-Peter Seidel, Hanspeter Pfister, Wojciech Matusik, Mohamed Elgharib, and Christian Theobalt. Lite2relight: 3d-aware single image portrait relighting. 2024. 3
- [37] Robin Rombach, Andreas Blattmann, Dominik Lorenz, Patrick Esser, and Björn Ommer. High-resolution image synthesis with latent diffusion models, 2021. 2, 3
- [38] Soumyadip Sengupta, Jinwei Gu, Kihwan Kim, Guilin Liu, David W Jacobs, and Jan Kautz. Neural inverse rendering of an indoor scene from a single image. In *Proceedings of the IEEE/CVF International Conference on Computer Vision*, pages 8598–8607, 2019. 2
- [39] Tiancheng Sun, Jonathan T Barron, Yun-Ta Tsai, Zexiang Xu, Xueming Yu, Graham Fyffe, Christoph Rhemann, Jay Busch, Paul Debevec, and Ravi Ramamoorthi. Single image portrait relighting. *ACM Transactions on Graphics (TOG)*, 38(4):1–12, 2019. 3
- [40] Shimon Vainer, Mark Boss, Mathias Parger, Konstantin Kutsy, Dante De Nigris, Ciara Rowles, Nicolas Perony, and Simon Donn e. Collaborative control for geometry-conditioned pbr image generation. *arXiv preprint arXiv:2402.05919*, 2024. 2
- [41] Shimon Vainer, Mark Boss, Mathias Parger, Konstantin Kutsy, Dante De Nigris, Ciara Rowles, Nicolas Perony, and Simon Donn e. Collaborative control for geometry-conditioned PBR image generation. In *European Conference on Computer Vision (ECCV)*, 2024. 3
- [42] Vikram Voleti, Chun-Han Yao, Mark Boss, Adam Letts, David Pankratz, Dmitry Tochilkin, Christian Laforte, Robin Rombach, and Varun Jampani. Sv3d: Novel multi-view synthesis and 3d generation from a single image using latent video diffusion. *arXiv preprint arXiv:2403.12008*, 2024. 2
- [43] Zhou Wang, A.C. Bovik, H.R. Sheikh, and E.P. Simoncelli. Image quality assessment: From error visibility to structural similarity. *IEEE Transactions on Image Processing*, 13(4): 600–612, 2004. 6
- [44] Zian Wang, Jonah Philion, Sanja Fidler, and Jan Kautz. Learning indoor inverse rendering with 3d spatially-varying lighting. In *Proceedings of the IEEE/CVF International Conference on Computer Vision*, pages 12538–12547, 2021. 2
- [45] Zhouxia Wang, Ziyang Yuan, Xintao Wang, Tianshui Chen, Menghan Xia, Ping Luo, and Yin Shan. Motionctrl: A unified and flexible motion controller for video generation. In *arXiv preprint arXiv:2312.03641*, 2023. 3
- [46] Jinbo Xing, Menghan Xia, Yong Zhang, Haoxin Chen, Wangbo Yu, Hanyuan Liu, Xintao Wang, Tien-Tsin Wong, and Ying Shan. Dynamicrafter: Animating open-domain images with video diffusion priors. *arXiv preprint arXiv:2310.12190*, 2023. 3
- [47] Zhongcong Xu, Jianfeng Zhang, Jun Hao Liew, Hanshu Yan, Jia-Wei Liu, Chenxu Zhang, Jiashi Feng, and Mike Zheng Shou. Magicanimate: Temporally consistent human image animation using diffusion model. In *arXiv*, 2023. 3
- [48] Hao-Hsiang Yang, Wei-Ting Chen, and Sy-Yen Kuo. S3Net: A Single Stream Structure for Depth Guided Image Relighting. In *2021 IEEE/CVF Conference on Computer Vision and Pattern Recognition Workshops (CVPRW)*, pages 276–283, Los Alamitos, CA, USA, 2021. IEEE Computer Society. 8
- [49] Renjiao Yi, Chenyang Zhu, and Kai Xu. Weakly-supervised single-view image relighting. In *Proceedings of the IEEE/CVF Conference on Computer Vision and Pattern Recognition (CVPR)*, pages 8402–8411, 2023. 2, 6, 7, 12
- [50] Ye Yu and William AP Smith. Inverserendernet: Learning single image inverse rendering. In *Proceedings of the IEEE/CVF Conference on Computer Vision and Pattern Recognition*, pages 3155–3164, 2019. 2
- [51] Chong Zeng, Yue Dong, Pieter Peers, Youkang Kong, Hongzhi Wu, and Xin Tong. DiLightNet: fine-grained lighting control for diffusion-based image generation. In *International Conference on Computer Graphics and Interactive Techniques*, 2024. 2, 3

- [52] Yan Zeng, Guoqiang Wei, Jiani Zheng, Jiabin Zou, Yang Wei, Yuchen Zhang, and Hang Li. Make pixels dance: High-dynamic video generation. *ArXiv*, abs/2311.10982, 2023. [3](#)
- [53] Lvmin Zhang, Anyi Rao, and Maneesh Agrawala. Adding conditional control to text-to-image diffusion models. In *Proceedings of the IEEE/CVF International Conference on Computer Vision*, pages 3836–3847, 2023. [2](#), [3](#), [4](#), [7](#)
- [54] Lvmin Zhang, Anyi Rao, and Maneesh Agrawala. Ic-light github page, 2024. [Online; accessed 20-May-2024]. [2](#), [3](#), [6](#), [7](#), [12](#)
- [55] Richard Zhang, Phillip Isola, Alexei A Efros, Eli Shechtman, and Oliver Wang. The unreasonable effectiveness of deep features as a perceptual metric. In *CVPR*, pages 586–595, 2018. [6](#)
- [56] Shangzhan Zhang, Sida Peng, Tao Xu, Yuanbo Yang, Tianrun Chen, Nan Xue, Yujun Shen, Hujun Bao, Ruizhen Hu, and Xiaowei Zhou. MaPa: text-driven photorealistic material painting for 3d shapes. In *International Conference on Computer Graphics and Interactive Techniques*, 2024. [3](#)
- [57] Xiao Zhang, William Gao, Seemantihar Jain, Michael Maire, David. A. Forsyth, and Anand Bhattad. Latent intrinsics emerge from training to relight, 2024. [2](#), [8](#), [12](#)

GenLit: Reformulating Single-Image Relighting as Video Generation

Supplementary Material

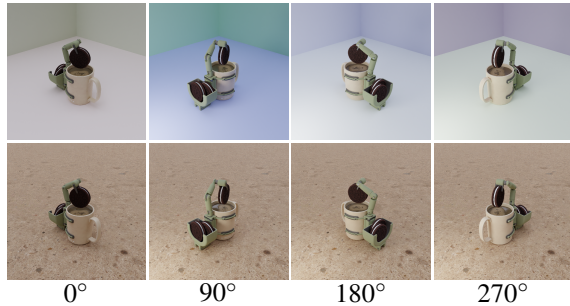


Figure 10. The same object is rendered under 4 orthogonal views under `wall-area` and `open-area` settings to emphasize the contrast in appearance.

7. Dataset

As mentioned in the main paper, we create our dataset using Blender 3.2.2 and render the scene with cycles. The objects in our videos are sourced from the Objaverse [9] dataset, spanning 945 LVIS [15] category annotations. To ensure high fidelity in geometry and materials, we filter the dataset to include only meshes with more than 4096 vertices and objects featuring more than four texture maps so that it includes albedo, perturbed normals and at least 2 texture maps for the material (metallic, diffuse, etc). Each object is rendered from four orthogonal views, rotated by 0° , 90° , 180° , and 270° along the z-axis as shown in Fig. 10. The point light at each frame is represented by a 5-D vector (see Section 3.2.1 in the main paper), and we create trajectories of 14 frames via linear interpolation of the polar coordinates. During the first four frames, the intensity of the environment map is dimmed from 1.0 to 0.4. Meanwhile, the intensity of the point light is increased from 0.0 at frame 1, to 75 lumens making it visible from frame 2. During the dimming process the position of the point light remains static; the light movement occurs between frames 5 and 14. Figure 12 shows 20 out of the 22 objects in the main test set (GENLIT-TEST), both for the `wall-area` setting (top four rows) and the `open-area` setting (bottom four rows).

8. Comparisons - Implementation Details

In the main paper we compare against two baselines that represent two different paradigms: IC-Light [54] (an inverse rendering baseline) and WS-SIR [49] (a reconstruction+rendering baseline). We adapt them to our setting as follows: For IC-Light, we render the background image of each test frame for `GenLit-Test.open-area` to exactly match the lighting of the ground truth relit image. We fol-

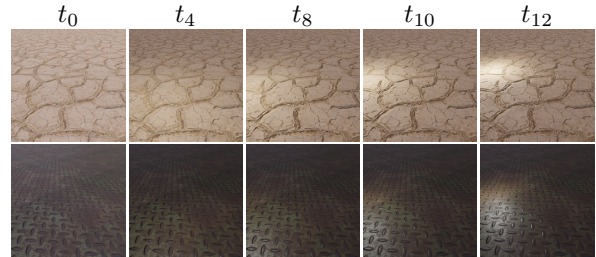


Figure 11. Implementation Details: Background images provided to IC-Light visualized at different frames. The generated background images match the lighting of each video.

low the dimming process and the movement of the point light as shown in Fig. 11. The input to the IC-Light network for each video is then the rendered background images for 14 frames, together with the input image (*i.e.* the original test image) along with the object mask. The background images are 768×768 pixels and we upsample the input image as IC-Light takes high resolution inputs.

For WS-SIR, we render HDRI maps for each frame of the video to match the lighting of the ground truth. We use a panoramic camera in Blender and create a sphere with an emissive material to represent the point light. We use the authors implementation to convert the HDRI maps to spherical harmonics. Further, we provide object mask to segment the albedo and normal maps prediction.

9. MIT Multi-Illumination Dataset

The MIT Multi-Illumination Dataset captures indoor scenes of the real world and has cluttered real-world objects composed of different materials. There are 945 scenes in the training set captured in different rooms such as the living room, kitchen, bathroom, etc. The test set has 30 scenes captured in different rooms, and the objects that appear in the test set are not part of the training set. Every scene is captured under 25 fixed lighting conditions, where the mounted light is rotated and the scene is lit by the light that bounces off the walls and ceilings. To adapt it to our setting, we consider each lighting condition as an input image and construct 25 trajectories where each trajectory has 14 light directions that are selected to form a continuous motion of light. We provide the order of the indices of each trajectory in Tab. 4. We downsample the images to size 512×768 . However, our quantitative comparisons against Latent-Intrinsics [57] in the main paper (Tab 3) is performed on the center cropped region of 512×512 for fairness.

Trajectories	Indices
1	[23, 11, 0, 10, 1, 17, 6, 15, 5, 13, 12, 4, 16, 14]
2	[14, 12, 4, 16, 15, 5, 13, 7, 11, 0, 10, 1, 17, 18]
3	[0, 11, 23, 24, 2, 22, 3, 19, 18, 17, 9, 8, 12, 13]
4	[11, 23, 24, 2, 22, 3, 19, 18, 17, 9, 8, 12, 13, 5]
5	[23, 24, 2, 22, 3, 19, 18, 17, 9, 8, 12, 13, 5, 15]
6	[24, 2, 22, 3, 19, 18, 17, 9, 8, 12, 13, 5, 15, 16]
7	[2, 22, 3, 19, 18, 17, 9, 8, 12, 13, 5, 15, 16, 4]
8	[12, 4, 16, 15, 5, 13, 7, 11, 0, 10, 1, 17, 18, 19]
9	[4, 16, 15, 5, 13, 7, 11, 0, 10, 1, 17, 18, 19, 3]
10	[16, 15, 5, 13, 7, 11, 0, 10, 1, 17, 18, 19, 3, 22]
11	[5, 13, 7, 11, 0, 10, 1, 17, 18, 19, 3, 22, 2, 24]
12	[1, 10, 0, 11, 23, 24, 2, 22, 3, 19, 18, 17, 9, 8]
13	[3, 19, 18, 17, 9, 8, 11, 7, 13, 5, 15, 16, 4, 14]
14	[6, 17, 1, 10, 0, 11, 23, 24, 2, 22, 20, 15, 16, 4]
15	[7, 11, 0, 10, 1, 17, 18, 19, 3, 22, 21, 13, 12, 4]
16	[8, 9, 17, 18, 19, 3, 22, 2, 24, 23, 11, 0, 10, 1]
17	[9, 8, 11, 23, 24, 2, 22, 3, 19, 18, 17, 9, 8, 12]
18	[10, 0, 11, 23, 24, 2, 22, 20, 15, 16, 4, 12, 13, 5]
19	[13, 5, 15, 16, 4, 12, 7, 24, 2, 22, 3, 19, 18, 17]
20	[17, 1, 10, 0, 11, 23, 24, 2, 22, 20, 15, 16, 4, 12]
21	[19, 20, 21, 24, 23, 11, 0, 10, 9, 16, 15, 5, 13, 12]
22	[20, 21, 24, 23, 11, 0, 10, 9, 16, 15, 5, 13, 12, 4]
23	[21, 24, 23, 11, 0, 10, 9, 16, 15, 5, 13, 12, 4, 14]
24	[22, 2, 24, 23, 11, 0, 10, 1, 18, 6, 15, 5, 13, 12]
25	[18, 19, 20, 21, 24, 23, 11, 0, 10, 9, 16, 15, 5, 13]

Table 4. We provide the indices of the light directions of the MIT dataset that are used to generate 25 different trajectories that are continuous. We ensure each light direction is fed as the input.

Obj	RMSE ↓	LPIPS ↓	SSIM ↑	PSNR ↑
50	0.039	0.015	0.967	30.376
100	0.045	0.015	0.966	29.343
150	0.038	0.014	0.968	30.608
200	0.046	0.015	0.967	29.166
270	0.037	0.016	0.967	30.960

Table 5. Results of training GenLit on 50, 100, 150 and 200 objects (wall-area setting).

10. Additional Experiments

10.1. Training with Less Objects

In the main paper we trained our models using a synthetic dataset containing 270 distinct objects. To measure the degree of generalization achieved by our model with varying amounts of training data, we investigated the performance loss incurred when the number of training objects is reduced. To this end, we evaluated four models on the wall-area setting, each trained with 50, 100, 150, and 200 objects, and compared them to our original setting of 270 objects using the GenLit-Test testing set (wall-area). We ensure that the size of each training set remains the same ($\sim 40k$) by increasing the number of

trajectories (*e.g.*, for 50 objects we sample 200 trajectories, while for 100 objects we sample 100 trajectories).

The results are shown in Table 5. Interestingly, the model trained on 50 objects performs almost as well as the one trained with the full 270 objects, with only relatively minor improvements in RMSE and PSNR for the 270-object case. This suggests that the model has a strong capacity to extrapolate observed light-material interactions from just a handful of objects.

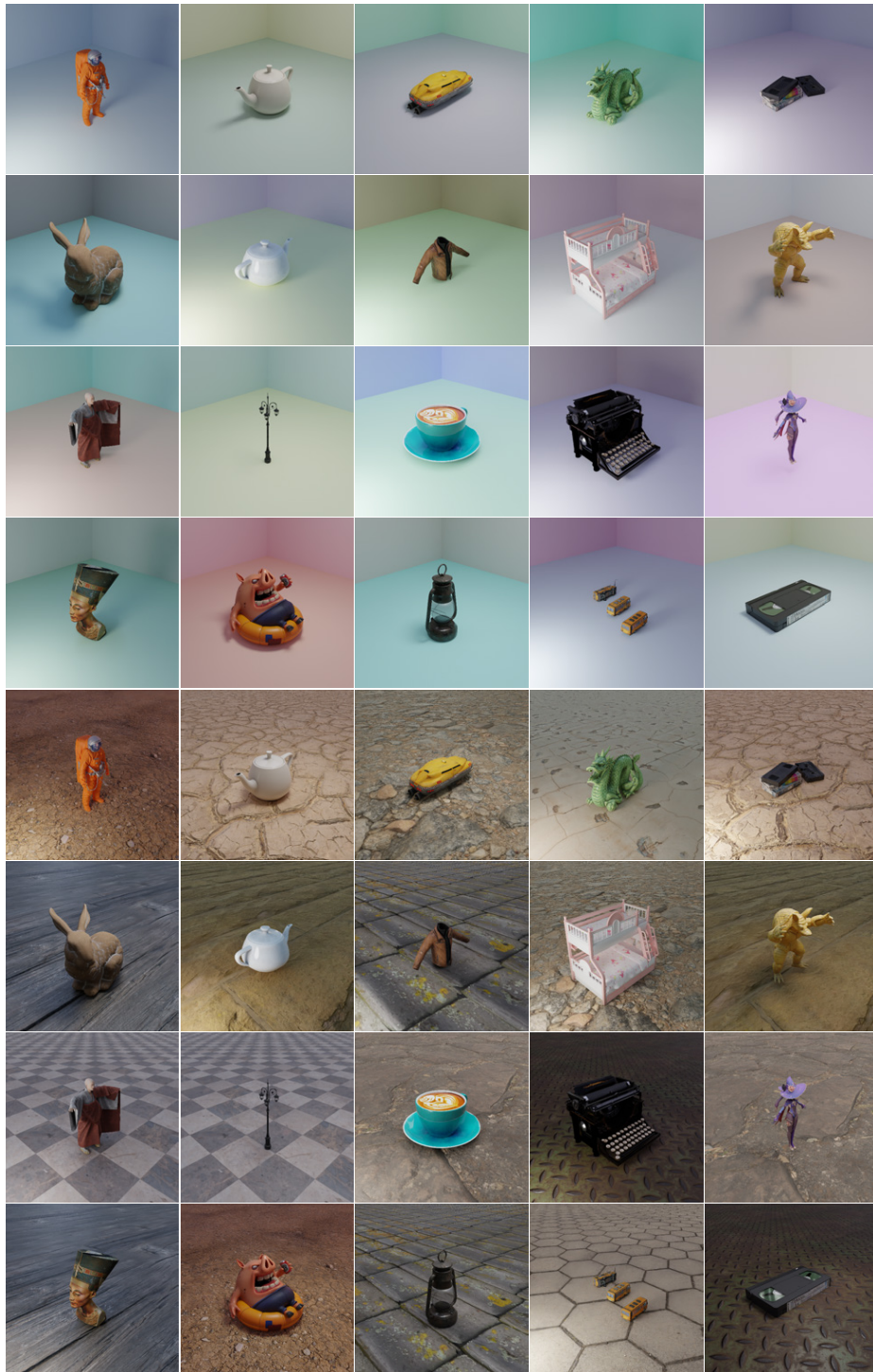


Figure 12. Visualization of 20 out of 22 test set objects rendered with the wall-area (top) and open-area setting (bottom).